energies

MDPI

Article

Investigation and Practical Application of Silica Nanoparticles Composite Underwater Repairing Materials

Jingbiao Yang [1], Shengxiang Deng [2,*], Hui Xu [3], Ye Zhao [4], Changda Nie [4] and Yongju He [3]

[1] School of Materials Science and Engineering, Central South University, Changsha 410083, China; yang_yjb@csu.edu.cn
[2] School of Mechanical and Automobile Engineering, Shanghai University of Engineering Science, Shanghai 201620, China
[3] Lab of Nano-Biology Technology, Institute of Super-Microstructure and Ultrafast Process in Advanced Materials, School of Physics and Electronics, Central South University, Changsha 410083, China; xuhui@csu.edu.cn (H.X.); heyongju@csu.edu.cn (Y.H.)
[4] School of Energy Science and Engineering, Central South University, Changsha 410083, China; 143901002@csu.edu.cn (Y.Z.); cdnie2018@csu.edu.cn (C.N.)
* Correspondence: csudsx@csu.edu.cn

Abstract: Repairing materials are well-known to play an important role in rehabilitating and extending the service life for hydraulic concrete structures. However, current underwater repairing materials possess several problems, including insufficient bond tensile strength, inconsistency with the deformation of the old substrate, and insufficient underwater self-sealing ability. In the present paper, an experimental study was carried out to evaluate the influence of silica nanoparticles (SNs) on the properties of underwater composite-repairing materials. The underwater deformation, impermeability, bond tensile strength, and compressive strength of the SN-modified underwater composite-repairing materials were used as the properties' evaluation indices. The results show that, within a certain range, the performance of the repairing material increase with increased SN percent. The deformability, impermeability grade, underwater bond tensile strength, and compressive strength of the SN-modified composite underwater repairing materials are 2.2%, 8, 2.91 MPa, and 115.87 MPa, respectively, when the mass ratio of the mortar, the curing agent and the SNs is 8:1:0.002. The proposed material is employed to repair the dam for a hydropower station in Guizhou province, China. Results show the seepage discharge is reduced by 8.6% when the dam is repaired. The annual average generating capacity is increased by 1.104 × 10^5 kWh. Meanwhile, CO_2 and NOx emissions are reduced by 1.049 × 10^5 and 220.8 kg annually, respectively.

Keywords: underwater repairing materials; silica nanoparticles; optimum mass ratio; economic analysis

check for updates

Citation: Yang, J.; Deng, S.; Xu, H.; Zhao, Y.; Nie, C.; He, Y. Investigation and Practical Application of Silica Nanoparticles Composite Underwater Repairing Materials. *Energies* **2021**, *14*, 2423. https://doi.org/10.3390/en14092423

Academic Editor: Idiano D'Adamo

Received: 23 March 2021
Accepted: 20 April 2021
Published: 23 April 2021

1. Introduction

Concrete is an indispensable material in water conservancy project construction and is very important for the safe operation of the whole project. Since the concretes are often exposed to many different loads—such as temperature change, water flow and sandiness stream, alternation of wet and dry, and freeze–thaw cycles—its members and structures are likely to experience serious defects, such as weathering, erosion, and carbonization [1,2]. These damages gradually accumulate over time and affect the safe working and service life of hydraulic structures [3]. Cracking is one of the most significant causes of deterioration in the durability of concrete structures [4,5], particularly for concrete in aqueous environments [6,7], where the working environment is bad. They need to be repaired in time after defects occur, otherwise they will have a serious impact on the safe use and durability of the whole structure [8]. According to an existing study [9], it is very time-consuming and significantly affects the economic efficiency to repair the cracks by emptying water; therefore, a proper material for repairing the underwater cracked concrete without water-emptying is needed.

Numerous studies have reported that the dispersion of nano-materials can significantly improve the mechanical and rheological properties of concretes [10–12]. Among various kinds of nano-materials, silica nanoparticles (SNs) and their derivatives are regarded as attractive candidates for reinforcing cement composites due to their high purity and specific surface area [13,14]. The SNs is also abundant and easy to produce. Miricioiu et al. [15,16] reported that the SN can be prepared from coal fly ash. Jamshidi et al. [17] pointed out that dispersing SNs into cement paste could lead to an increase in cohesion, plastic viscosity, and yield stress. Potapov et al. [18] demonstrated that dispersing SNs could reduce the pore connectivity and increase the pore refining in cement mixtures, which significantly reduces the permeability of cement-based materials. The principle of enhancement is that dispersing SNs could extend pozzolanic reactivity and form a substantial amount of calcium–silicate–hydrate (C–S–H) gel [19,20]. Makarova et al. [21] evaluated the effect of SNs on the mechanical properties of plain concrete. It was reported that the strength of concrete with SNs was increased by 84, 93, and 35% after 3, 7, and 28 days, respectively. Grzeszczyk et al. [22] reported that dispersing SNs can improve the washout of concrete and has no significant effect on compressive strength. Khaloo et al. [23] explored the performance of concrete dispersed with SNs in different specific surface areas. It was found that SNs with a lower specific surface area performed better than the higher one in compressive, splitting tensile strengths and electrical resistivity. Raheem et al. [24] reviewed the effect of the incorporation of SNs in blended cement mortar and concrete. It was concluded that SNs have been shown to fill the micropores in concrete and improve its microstructural arrangement, thus producing high-density concrete.

Repairs of the underwater concrete structures are complicated construction works due to the constant dynamic action of water on these structures. It has been reported that a material used to repair concrete cracks in dry conditions is invalid in the underwater condition since it often fails to bond to the damaged concrete and adverse effects can occur with the reaction between the hardener and the water [25,26]. For example, the curing agent in epoxy mortar reacts with water and carbon dioxide, which leads to a sharp decrease in bond strength [27]. It was reported that the underwater repairs had shown slightly inferior ultimate strengths and peak load displacement [28]. Shi et al. [29] investigated the effect of humidity on the mechanical properties of polymer-modified, cement-based repair materials. Results showed that the compressive strength decreased under different humidity-curing conditions. Li et al. [30] prepared a new cementitious anti-washout grouting material (CIS), which consists of ordinary Portland cement, coagulant accelerator water glass, and flocculating agent xanthan gum. Liao et al. [25] conducted a large-scale experimental study on bond behavior between polymer-modified cement mortar layer and concrete. Assaad et al. [31] conducted a comprehensive research study to evaluate the effect of styrene-butadiene rubber (SBR) latex admixture on the washout loss and bond strength of underwater concrete designated for repair applications.

This literature review shows that SNs can effectively seal the cracks and pores within the structure of repairing materials, which is attributed to the good uniformity of SNs that make the microstructure of repairing materials more dense. However, previous studies of SNs on concrete mainly focused on the properties and microstructure; the study of the application of SNs for the underwater repair of cracked concrete has not been conducted yet. This study is carried out to address this issue. The effect of SNs on the repair of the underwater composite material was investigated experimentally. The performance of the SN-modified underwater composite-repairing material, including the deformability, impermeability grade, underwater bond tensile strength, and compressive strength, were measured for four different SNs additive ratios, and an optimum mass ratio of mortar, curing agent, and SN was achieved. Moreover, a hydropower station was repaired using the optimum mass ratio of SN-modified underwater composite-repairing material, and the economic and environmental benefits were analyzed. These results would be beneficial for broad underwater concrete repair applications, such as for dams of hydropower stations, piles in a marine environment, and sea walls.

2. Materials and Methods

2.1. Materials

SN-modified underwater composite-repairing material is a kind of polymer slurry, which mainly consists of mortar, silica nanoparticles, and a curing agent. The mortar was made by our study team using the components listed in Table 1, which were provided by Changsha Shengkang Polymer Material Technology Co., Ltd., Changsha, China. The Mortar was prepared using: Portland cement CEM I 42.5R with a density of 3100 kg/m^3 and a Blaine fineness of 335 m^2/kg; river sand with a grain size of up to 1 mm and coarse aggregates consisting of crushed stones, which had a maximum size of 6 mm; an F type of fly ash; Bisphenol A-based Epoxy Resins and superplasticizer, provided by Wuxi Huaou Chemical Technology Co., Ltd., Wuxi, China; and water. The chemical composition of CEM I 42.5R is listed in Table 2. The Silica nanoparticles were produced by our study team and had a specific surface area between 60 and 400 m^2/g and nanoparticles sizes between 5 nm and 100 nm. The thermo-setting of this material was initiated by a curing agent (Sinopharm Chemical Reagent Co., Ltd., Shanghai, China).

Table 1. Mixture proportions of mortar (Unit: kg).

Material	CEM I 42.5R	River Sand	Fly Ash Type F	Superplasticizer	Crushed Stone	Epoxy Resins	Polymer Adhesive
Consumption	429	866	57	7.6	1024	28	24

Table 2. Chemical compositions of CEM I 42.5R.

Component	SiO_2	Al_2O_3	Fe_2O_3	CaO	MgO	K_2O	Na_2O	SiO_3
Weight (%)	19.8	6.2	2.6	63.2	1.3	0.8	0.7	2.9

2.2. Specimen Preparation

Four different mass ratios of the above-mentioned materials were investigated, as listed in Table 3. First, mortar, the curing agent, and SNs with different mass ratios were stirred for several minutes until the color of the mixture was uniform and there were no lumps existing in the mixture. Second, in order to remove the air entrained during the stirring process, the mixtures were set aside for 5 min. Finally, SN-modified underwater composite-repairing materials with four formulations (F1, F2, F3, F4) were obtained to evaluate their influences on the repair of the underwater cracked concrete.

Table 3. Formulations of silica nanoparticle (SN)-modified underwater composite-repairing material.

Formulations	Mortar: Curing Agent: SN Mass Ratio
F1	8: 1: 0.0020
F2	8: 1: 0.0015
F3	8:1:0.0010
F4	8:1:0

For the deformability test, SN-modified underwater composite-repairing material specimens, with dimensions of 70.7 × 70.7 × 70.7 mm^3, were prepared. Then, these specimens were cured in water for 15 days. Finally, a cylinder core specimen with a diameter of 49.0 mm and a height of 50.0 mm was taken out, as shown in Figure 1a.

For the impermeability test, SN-modified underwater composite-repairing materials were poured into truncated cone barrels (175 × 185 × 150 mm^3), as shown in Figure 1b. After the SN-modified materials had solidified, the specimens were taken out of the barrels and cured in water for 7 days. The side face of the clean-wiped, and the truncated cone impermeability specimen was scribbled by a layer of molten paraffin. Then, the specimen was pressed into the preheated barrel by a screw presser. After drying, the split between the model and the barrel was sealed with mortar and butter.

To evaluate the composite behavior and bonding effect between SN-modified materials and concrete structural members, a pull-out test was conducted. Four concrete blocks ($100 \times 100 \times 100$ mm^3) and four slotted concrete blocks ($100 \times 100 \times 100$ mm^3) with center openings of 10 mm width and 80 mm depth were prepared. These concrete blocks were grouted with SN-modified materials in the underwater condition (50 m deep) and the pouring height was 80 mm. After 15 days of water curing, a cylinder core specimen with a diameter of 49 mm and a height of 100 mm was taken out, as shown in Figure 1c.

To evaluate the compressive strength of the SN-modified underwater composite-repairing materials, $40 \times 40 \times 40$ mm^3 hexahedron specimens were prepared, as shown in Figure 1d. Afterward, these specimens were cured in water for 15 days.

(**a**) (**b**) (**c**) (**d**)

Figure 1. Test specimens of the SN-modified underwater composite-repairing material: (**a**) deformability; (**b**) impermeability; (**c**) bond strength; (**d**) compressive strength tests.

2.3. Test Method and Instrument

These cylinder core specimens were mounted on a testing machine (MTS Landmark, MTS Instrument Inc., Eden Prairie, MN, USA) for the deformability test (Figure 2a). The loading rate of the MTS was 0.15 mm/min, displacement-controlled. Before mounting the specimen on the impermeability tester, the impermeability tester was started and the valves under the six test positions were opened until the water seeped out of the six holes and filled the test pit (Figure 2b, Crew pressurizer, Tianjin experimental instrument factory, China). These specimens with bond strength tests were mounted on the MTS Landmark using the resin adhesive (Figure 2c). The loading rate of the UTM was 0.75 kN/min (0.4 MPa/min), force-controlled. Figure 2d shows the 150tCH-5 pressure testing machine (Hebei Luyuan Jianyi Test Instrument Co., Ltd., Hebei, China) with a design pressure of 150 MPa.

(**a**) (**b**) (**c**) (**d**)

Figure 2. Overall photo of test setup: (**a**) deformability; (**b**) impermeability; (**c**) bond strength; (**d**) compressive strength tests.

3. Results and Discussion

3.1. Performance Analysis

Experimental results regarding the deformability of SN-modified underwater composite-repairing materials are summarized in Table 4. It is seen that SN-modified materials have better deformability when compared to the traditional material. With the increase in the concentration of the SN component, the deformability of the SN-modified underwater composite-repairing materials was increased. When compared to the material without SNs (F4), the deformability of F1 was increased by 46.7%. This means that the addition of SNs significantly improves the deformability of traditional underwater repairing materials.

Table 4. Deformability of SN-modified underwater composite-repairing materials.

Formulations	Diameter (mm)	Height (mm)	Peak Load (kN)	Tensile Stress (MPa)	Maximum Tensile Length (mm)	Deformability (%)
F1	49.03	53.11	8.23	4.40	1.24	2.2
F2	49.07	53.11	8.23	4.40	1.24	2.0
F3	49.04	53.11	8.23	4.38	1.22	1.8
F4	49.05	53.11	8.23	4.36	1.23	1.5

Table 5 summarizes the test results of impermeability. The determination of the impermeability grade (P) was written as $P = 10H - 1$, where H was the water pressure when three of the six models were seeped. The increased ratio of water pressure was 0.1 MPa, and the test time was eight hours for every water pressure level. It was found that the impermeability of F1 was the highest, followed by F2, F3, and F4. For the specimen of F1, the impermeability was 8th grade. This means that the SN-modified underwater composite-repairing materials can decrease the risk of cracking concrete and improve service life.

Table 5. Impermeability of SN-modified underwater composite-repairing materials.

Formulations	F1	F2	F3	F4
Impermeability Grade	8	8	7	6

Table 6 provides the test results of tensile bond strength. It can be seen that when compared with repairing materials containing no SN, SN-modified underwater composite-repairing materials have a higher underwater tensile bond strength. Underwater tensile bond strength increased as SN percent increased. The tensile bond strength of F1, with and without cracks, was 2.91 and 3.05 MPa, respectively. The results showed that the retrofitting of damaged RC structures using the SN-modified material is effective. Figure 3 shows the debonding failure of the sample of F1 without cracks. It is seen that the debonding failure occurs in the interface of concrete and fixed support.

Table 6. Tensile bond strength of SN-modified underwater composite-repairing materials.

Formulations	F1 [a]	F2 [a]	F3 [a]	F4 [a]	F1 [b]	F2 [b]	F2 [b]	F4 [b]
Diameter (mm)	49.00	49.03	49.02	49.05	49.08	49.07	49.06	49.03
Bond Tensile Strength (MPa)	3.05	2.88	2.85	2.21	2.91	2.74	2.52	2.11

[a] Interfacial bonding; [b] concrete cracking.

Table 7 gives the test results for compressive strength. It could be seen that the compressive strength of underwater repairing materials increased as SN percent increased. The compressive strength of F1 is the highest, at 115.87 MPa, and increased by 17.3%

compared to F4. The results showed that the retrofitting of damaged RC structures using the SN-modified material is effective.

Table 7. Compressive strength of the SN-modified underwater composite-repairing materials.

Formulations	F1	F2	F3	F4
Pressure (kN)	185.39	180	170.91	158
Compressive Strength (MPa)	115.87	112.50	106.82	98.75

(**a**) (**b**)

Figure 3. Debonding failures of the sample of F1 without cracks (**a**) lower end-face; (**b**) upper end-face.

By comparing the relationships between the above four parameters, it was found that among the four materials, the specimen of F1 has the best performance. For the repairing material without SNs, underwater bond tensile strength, deformability, impermeability grade, and compressive strength were 2.21 MPa, 1.5%, 6, and 98.75 MPa, respectively. The SN-modified underwater composite-repairing material showed an underwater bond tensile strength of 2.91 MPa, deformability of 2.2%, an impermeability grade of 8, and a compressive strength of 115.87 MPa, respectively, when the mass ratio of mortar, the curing agent, and SNs was 8:1:0.002. This is because the SNs decreased the pore volume of the concrete, as shown in Figure 4, which displays typical scanning electron microscopy (SEM) images of the SN-modified underwater composite-repairing material. It is obvious that SN-modified underwater composite-repairing materials are uniform spheres with an average size of 100 nm. It clearly shows that unconsumed spherical agglomerated SNs (white particles) still exist and that the dispersion of SNs is relatively uniform. The phenomenon can better achieve the pozzolanic reactivity, nucleation effect, and filling effect of SNs. It is also seen that the internal structure of the mortar is very compact, which results in high bonding strength and low permeability of the repairing material.

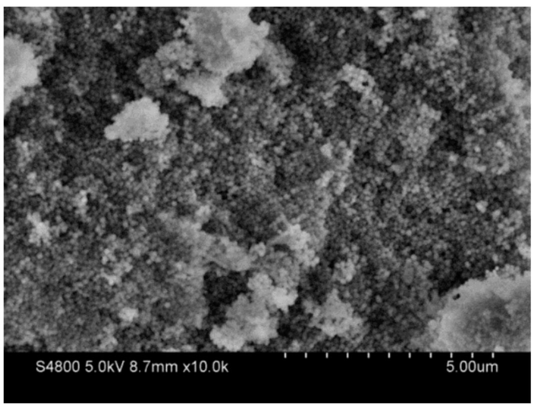

Figure 4. The SEM image of the SN-modified underwater composite-repairing material.

3.2. *Engineering Application*

3.2.1. Engineering Case

The SN-modified underwater composite material was used to repair a hydropower station. The installed capacity of this hydropower station is 1000 MW, and the annual average generating capacity is 2.428 × 10^9 kWh. The hydropower station has a main dam and an auxiliary dam with an annual average water flow of 240 m^3/s. The main dam has dimensions of 185.5 m height and 423.75 m length, and the auxiliary dam has dimensions of 92.13 m height and 233.72 m length. The dam is made of concrete and pouring in three time stages. In 2017, the dam was damaged and infiltration occurred. In order to fully understand the damage status of the dam, the power plant conducted an underwater video inspection of the dam in May 2017. It was observed that there was an obvious crack in the joint area of the main dam in phase I and phase II, and parts of the wall were hollowed out by high-speed flow, as shown in Figure 5.

(**a**) (**b**)

Figure 5. Pictures of the damaged condition of (**a**) joint area; (**b**) partial enlarged drawing.

The underwater tremie placement technology was used to pour underwater concrete to repair the side wall. Firstly, the size and damage of the panning hole were measured. Secondly, the damaged side wall was cleaned, cut, and polished, and other pre-processing was completed. Thirdly, an anchor bar and weld steel mesh were inserted, which enhances the bond between the bottom plate and the repair material. Then, steel formwork was erected, which can maintain the repair material molding and curing. Finally, the side wall was drilled and then grouted (Figure 6).

(**a**) (**b**) (**c**) (**d**)

Figure 6. The construction process: (**a**) panel cutting; (**b**) die fixing; (**c**) construction panel drilling; (**d**) grouting.

3.2.2. Economic Analysis

Figure 7 shows the statistical data for the upstream water level and the seepage discharge. It should be mentioned that the repair work was conducted in May 2017. That is to say, the dam was not repaired before May. It is seen that the upstream water levels in March and June 2017 are nearly the same, and the seepage discharge in June (116.51 L/s) is obviously lower than that shown for March (127.43 L/s). This indicates that the seepage discharge was reduced by 8.6%.

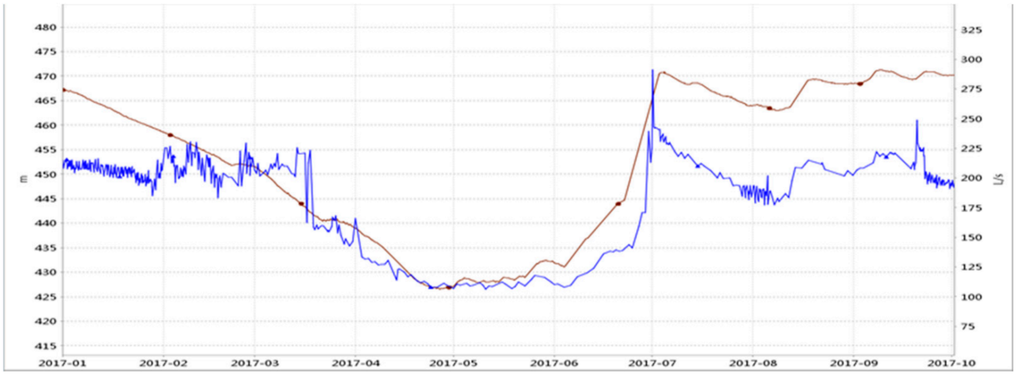

Figure 7. Statistical data for the upstream water level (red line) and the seepage discharge (blue line).

Decreasing the average seepage discharge of the dam can increase the generating capacity of the hydropower station. The increase in generating capacity (C) can be calculated by the following equation:

$$C = \Delta S \times \frac{W}{Q \times t} \quad (1)$$

where W is the annual average generating capacity (2.428×10^9 kWh), Q is the annual average water flow (240 m^3/s), ΔS is the average seepage discharge difference between after and before the dam repair (0.0109 m^3/s), and t is time (s).

It can be calculated that the annual average generating capacity is increased by 1.104×10^5 kWh when the dam is repaired. The on-grid price is 0.36 RMB/kWh in the hydropower station. Therefore, the annual revenue from the increase in power generation is 39,800 RMB.

Hydropower is a clean and renewable energy source and can reduce greenhouse gas emissions. It was reported that the production of 1 kWh of electricity of thermal power needs about 0.3 kg of coal [32], which releases about 0.950 kg of CO_2 [33,34] and 0.002 kg of NO_x [35,36] into the atmosphere. That is to say, CO_2 and NO_x emissions are reduced by 1.049×10^5 and 220.8 kg, respectively, and 3.312×10^4 kg of coal is saved annually when the dam is repaired using the SN-modified underwater composite material. It can be concluded that the underwater material proposed can both increase economic benefits and reduce greenhouse gas emissions.

4. Conclusions

In the present study, the SN was used as an additive during the preparation of underwater composite-repairing material. It is found that the tensile strength, deformability, and impermeability of the modified repairing materials dispersed with SNs are significantly increased, which can meet the repairing requirement of underwater concrete. The influence of SNs on the properties of the modified underwater composite-repairing material was evaluated by adding four different mass ratios of SNs. It is found that these above performances are enhanced with the increase in the SN mass fraction. Moreover, the proposed underwater repairing material was used in a hydropower station. Results show that the seepage discharge is significantly reduced when the dam is repaired, which significantly increases economic benefits and reduces greenhouse gas emissions.

Author Contributions: Conceptualization, S.D. and J.Y.; methodology, S.D. and H.X.; investigation, Y.H.; data curation, Y.Z.; writing—original draft preparation, J.Y.; writing—review and editing, S.D. and C.N.; supervision, H.X.; project administration, Y.H. and Y.Z. All authors have read and agreed to the published version of the manuscript.

Funding: This research received no external funding.

Institutional Review Board Statement: Not applicable.

Informed Consent Statement: Not applicable.

Data Availability Statement: The data presented in this study are available on request from the corresponding author.

Acknowledgments: We thank the Wuling Power Sanbanxi Hydropower Plant for their guidance and help.

Conflicts of Interest: The authors declare no conflict of interest

References

1. Abid, S.R.; Hilo, A.N.; Ayoob, N.S.; Daek, Y.H. Underwater abrasion of steel fiber-reinforced self-compacting concrete. *Case Stud. Constr. Mater.* **2019**, *11*, e00299. [CrossRef]
2. Zhang, B.; Gao, F.; Zhang, X.; Zhou, Y.; Hu, B.; Song, H. Modified cement-sodium silicate material and grouting technology for repairing underground concrete structure cracks. *Arab. J. Geosci.* **2019**, *12*, 4–13. [CrossRef]
3. Horszczaruk, E.; Brzozowski, P. Effects of fluidal fly ash on abrasion resistance of underwater repair concrete. *Wear* **2017**, *376–377*, 15–21. [CrossRef]
4. Lyu, Z.; Shen, A.; Mo, S.; Chen, Z.; He, Z.; Li, D.; Qin, X. Life-cycle crack resistance and micro characteristics of internally cured concrete with superabsorbent polymers. *Constr. Build. Mater.* **2020**, *259*, 119794. [CrossRef]
5. Duan, P.; Yan, C.; Luo, W. A novel waterproof, fast setting and high early strength repair material derived from metakaolin geopolymer. *Constr. Build. Mater.* **2016**, *124*, 69–73. [CrossRef]
6. Yi, N.H.; Nam, J.W.; Kim, S.B.; Kim, I.S.; Kim, J.H.J. Evaluation of material and structural performances of developed Aqua-Advanced-FRP for retrofitting of underwater concrete structural members. *Constr. Build. Mater.* **2010**, *24*, 566–576. [CrossRef]
7. Zhuang, N.; Dong, H.; Zhou, Y.; Chen, D. Cracking behavior of reinforced concrete piles externally bonded with carbon fiber reinforced polymer in a marine environment. *Constr. Build. Mater.* **2018**, *190*, 1154–1162. [CrossRef]
8. Chu, H.; Liang, Y.; Guo, M.Z.; Zhu, Z.; Zhao, S.; Song, Z.; Wang, L.; Jiang, L. Effect of electro-deposition on repair of cracks in reinforced concrete. *Constr. Build. Mater.* **2020**, *238*, 117725. [CrossRef]
9. Horszczaruk, E.; Brzozowski, P. Bond strength of underwater repair concretes under hydrostatic pressure. *Constr. Build. Mater.* **2014**, *72*, 167–173. [CrossRef]
10. Singh, N.B.; Kalra, M.; Saxena, S.K. Nanoscience of Cement and Concrete. *Mater. Today Proc.* **2017**, *4*, 5478–5487. [CrossRef]
11. Hanif, A. Reinforcing cementitious composites with graphene oxide for enhanced mechanical performance. In *Smart Nanoconcretes and Cement-Based Materials*; Elsevier: Amsterdam, The Netherlands, 2020; pp. 619–635. [CrossRef]
12. Nazar, S.; Yang, J.; Thomas, B.S.; Azim, I.; Ur Rehman, S.K. Rheological properties of cementitious composites with and without nano-materials: A comprehensive review. *J. Clean. Prod.* **2020**, *272*, 122701. [CrossRef]
13. Hou, P.; Shi, J.; Prabakar, S.; Cheng, X.; Wang, K.; Zhou, X.; Shah, S.P. Effects of mixing sequences of nanosilica on the hydration and hardening properties of cement-based materials. *Constr. Build. Mater.* **2020**, *263*, 120226. [CrossRef]
14. Yang, H.; Monasterio, M.; Zheng, D.; Cui, H.; Tang, W.; Bao, X.; Chen, X. Effects of nano silica on the properties of cement-based materials: A comprehensive review. *Constr. Build. Mater.* **2021**, *282*, 122715. [CrossRef]
15. Miricioiu, M.G.; Niculescu, V.C. Fly ash, from recycling to potential raw material for mesoporous silica synthesis. *Nanomaterials* **2020**, *10*, 474. [CrossRef]
16. Miricioiu, M.G.; Niculescu, V.C.; Filote, C.; Raboaca, M.S.; Nechifor, G. Coal fly ash derived silica nanomaterial for mmms-application in CO_2/CH_4 separation. *Membranes* **2021**, *11*, 78. [CrossRef]
17. Jamshidi, A.; Kurumisawa, K.; White, G.; Jize, M.; Nawa, T. Use of nanotechnology in concrete pavements. In *Smart Nanoconcretes and Cement-Based Materials*; Elsevier: Amsterdam, The Netherlands, 2019; pp. 384–401. [CrossRef]
18. Potapov, V.; Efimenko, Y.; Fediuk, R.; Gorev, D. Effect of hydrothermal nanosilica on the performances of cement concrete. *Constr. Build. Mater.* **2021**, *269*, 121307. [CrossRef]
19. Paul, S.C.; van Rooyen, A.S.; van Zijl, G.P.; Petrik, L.F. Properties of cement-based composites using nanoparticles: A comprehensive review. *Constr. Build. Mater.* **2018**, *189*, 1019–1034. [CrossRef]
20. She, W.; Du, Y.; Miao, C.; Liu, J.; Zhao, G.; Jiang, J.; Zhang, Y. Application of organic- and nanoparticle-modified foams in foamed concrete: Reinforcement and stabilization mechanisms. *Cem. Concr. Res.* **2018**, *106*, 12–22. [CrossRef]
21. Makarova, N.V.; Potapov, V.V.; Kozin, A.V.; Chusovitin, E.A.; Amosov, A.V.; Nepomnyashiy, A.V. Influence of hydrothermal nanosilica on mechanical properties of plain concrete. *Key Eng. Mater.* **2017**, *744*, 126–130. [CrossRef]
22. Grzeszczyk, S.; Jurowski, K.; Bosowska, K.; Grzymek, M. The role of nanoparticles in decreased washout of underwater concrete. *Constr. Build. Mater.* **2019**, *203*, 670–678. [CrossRef]
23. Khaloo, A.; Mobini, M.H.; Hosseini, P. Influence of different types of nano-SiO_2 particles on properties of high-performance concrete. *Constr. Build. Mater.* **2016**, *113*, 188–201. [CrossRef]

24. Raheem, A.A.; Abdulwahab, R.; Kareem, M.A. Incorporation of metakaolin and nanosilica in blended cement mortar and concrete- A review. *J. Clean. Prod.* **2021**, *290*, 125852. [CrossRef]
25. Liao, W.; Wang, H.; Li, M.; Ma, C.; Wang, B. Large scale experimental study on bond behavior between polymer modified cement mortar layer and concrete. *Constr. Build. Mater.* **2019**, *228*, 116751. [CrossRef]
26. Hong, S.; Park, S.K. Behavior of concrete columns repaired with polymer mortar and epoxy fiber panel. *Adv. Mater. Sci. Eng.* **2013**, *2013*, 748294. [CrossRef]
27. Lu, Z. Applicability of Epoxy Materials for Repairing Wet and Underwater Concrete. *IOP Conf. Ser. Earth Environ. Sci.* **2020**, *598*, 012019. [CrossRef]
28. George, J.M.; Kimiaei, M.; Elchalakani, M.; Fawzia, S. Experimental and numerical investigation of underwater composite repair with fibre reinforced polymers in corroded tubular offshore structural members under concentric and eccentric axial loads. *Eng. Struct.* **2021**, *227*, 111402. [CrossRef]
29. Shi, C.; Zou, X.; Yang, L.; Wang, P.; Niu, M. Influence of humidity on the mechanical properties of polymer-modified cement-based repair materials. *Constr. Build. Mater.* **2020**, *261*, 119928. [CrossRef]
30. Li, S.; Zhang, J.; Li, Z.; Gao, Y.; Qi, Y.; Li, H.; Zhang, Q. Investigation and practical application of a new cementitious anti-washout grouting material. *Constr. Build. Mater.* **2019**, *224*, 66–77. [CrossRef]
31. Assaad, J.J.; Gerges, N.; Khayat, K.H.; Lattouf, N.; Mansour, J. Assessment of bond strength of underwater polymer-modified concrete. *ACI Mater. J.* **2019**, *116*, 169–178. [CrossRef]
32. Guttikunda, S.K.; Jawahar, P. Atmospheric emissions and pollution from the coal-fired thermal power plants in India. *Atmos. Environ.* **2014**, *92*, 449–460. [CrossRef]
33. Nagarkatti, A.; Kolar, A.K. Assessment of Life Cycle Greenhouse Gas Emissions from Coal Fired Power Plants in India. *Appl. Mech. Mater.* **2014**, *704*, 487–490. [CrossRef]
34. Kreutz, T.; Williams, R.; Consonni, S.; Chiesa, P. Co-production of hydrogen, electricity and CO_2 from coal with commercially ready technology. Part B: Economic analysis. *Int. J. Hydrog. Energy* **2005**, *30*, 769–784. [CrossRef]
35. Nazari, S.; Shahhoseini, O.; Sohrabi-Kashani, A.; Davari, S.; Paydar, R.; Delavar-Moghadam, Z. Experimental determination and analysis of CO_2, SO_2 and NOx emission factors in Iran's thermal power plants. *Energy* **2010**, *35*, 2992–2998. [CrossRef]
36. Shi, Y.; Xia, Y.F.; Lu, B.H.; Liu, N.; Zhang, L.; Li, S.J.; Li, W. Emission inventory and trends of NO x for China, 2000–2020. *J. Zhejiang Univ. Sci. A* **2014**, *15*, 454–464. [CrossRef]